Electronic Supplementary Material (ESI) for Physical Chemistry Chemical Physics.

# *A tool for deciphering the redox potential ranking of organic compounds: the case study of biomass extracted quinones for sustainable energy*

Electronic Supplementary Information (ESI)

Phys. Chem. Chem. Phys., (2020), DOI: 10.1039/d0cp02045a.

Fanny Lambert,[a] Yann Danten [b] and Carlo Gatti [c] and Christine Frayret,*[a]

[a.] *Laboratoire de Réactivité et Chimie des Solides (LRCS), UMR CNRS 7314, Université de Picardie Jules Verne, Hub de l'Energie, 15 Rue Baudelocque, 80000 Amiens Cedex, France. Réseau sur le Stockage Electrochimique de l'Energie (RS2E), FR CNRS 3459, France. *E-mail: christine.frayret@u-picardie.fr*

[b.] *Institut des Sciences Moléculaires, UMR CNRS 5255, 351 Cours de la Libération, 33405 Talence, France.*

[c.] *CNR SCITEC, CNR Istituto di Scienze e Tecnologie Chimiche "Giulio Natta", Sede Via C. Golgi, 19,20133 Milano, Italy.*

## Supplementary Information

## 1.1 Complete structural description along with ESP analysis of DOPA, Cl-DOPA, *L*-DOPA, CQ and HMQ (corresponding Figures and further explanations are provided in section 1.2 and 1.3)

### *DOPA and Cl-DOPA*

The calculated PES (provided in SI, Fig. SI-6) have demonstrated that DOPA and Cl-DOPA molecules are characterized by three local energy-minimum structures (conformers) due to possible orientations of the $(CH_2)_2$-$NH_2$ group with respect to the plane of the 6MR. For the initial form (monomer), the most stable Structure, A (*c.f.* SI), corresponds to the $(CH_2)_2$-$NH_2$ group being positioned nearly in coincidence with the plane of the 6MR (*i.e.* in plane (*i.p.*) configuration). The ESP map of the most stable configuration of the initial DOPA system exhibits two minima, at -59.01 and -28.70, the most important one in absolute value being in the vicinity of the redox centres (again at half-way from the two O) while the second one is located nearby the end of the functional group. The two other conformations (structures B and C) correspond instead to *out of plane* (*o.p.*) positioning of the $(CH_2)_2$-$NH_2$ group (*c.f.* SI). With respect to Cl-DOPA, the ESP map of the initial system behaves very similarly compared to the DOPA with the most important minimum placed in between the two Oxygen atoms (-53.57) and the other one near the functional group (-29.29). In contrast to the initial states for DOPA and Cl-DOPA, PES analyses (*c.f.* SI) indicate that in the case of the intermediate forms or the final form of Mg-based system of these compounds, both structures with *o.p.* $(CH_2)_2$-$NH_2$ conformations become more stable than the corresponding *i.p.* $(CH_2)_2$-$NH_2$ orientation. The substitution of an H-atom with a Cl-atom on the *o*-quinone ring also favours a more stable structure with the *o.p.* $(CH_2)_2$-$NH_2$ conformation but having an opposite orientation comparatively to that in the intermediate form of DOPA (conformation C, *c.f.* Fig. SI-6). The calculated interatomic distances involved in the bidentate interaction between alkaline atom (Li or Na) or Mg species and both Oxygen atoms from the two redox centres attached to the 6MR are comparable to those evaluated for the IQ (*i.e.* 1.86 Å, 2.21 Å,1.91 Å for Li-, Na- and Mg-based systems in the case of DOPA and 1.87 Å, 2.21 Å,1.91 Å for Cl-DOPA). In final forms involving $Li^+$ or $Na^+$ cations, two possible locations can naturally be envisioned for the further alkaline ion according to the side selection of this cation. The most stable final structure for the DOPA is the one involving the additional alkaline species interacting with the C=O group of the ring separated from the $(CH_2)_2$-$NH_2$ chain (in conformation B) by the two consecutive CH bonds, as expected from the ESP maps (with a value of -36.12/-40.28 against -35.90/-39.85 on the other side for $Li^+$/$Na^+$, respectively). In the most stable final form of DOPA, the bidentate interaction involves the following interatomic distances between O and alkaline cations are observed: (1.79 Å/1.84 Å) and (2.15 Å/2.18 Å) for $Li^+$ and $Na^+$, respectively, the additional interatomic distance involving the supplementary alkaline cation being equal to : 1.75 Å (Li)/2.11 Å (Na) for these two systems. In Cl-DOPA, such values are very similar and correspond to: (1.80 Å/1.84 Å) and (2.15 Å/2.19 Å) in the bidentate interaction and 1.76 Å (Li)/2.11 Å (Na) for the further interaction. The ESP map of the Cl-DOPA intermediate system exhibits two minima which are less differentiated than most other cases (-31.43 and -31.85 for $Li^+$; -35.78 and -35.36 for $Na^+$) and the final form of this entity corresponds in fact to the additional alkaline species interacting with the C=O group of the ring separated from the $(CH_2)_2$-$NH_2$ chain (in conformation C) by only one CH bond. For both DOPA and Cl-DOPA, the secondary structures in final form correspond to a reciprocal arrangement of the additional alkaline with respect to C=O groups comparatively to the most stable structure (*c.f.* Fig. SI-7). Actually, the Gibbs free energy difference $\Delta G$ between both structures is relatively weak for a given compound, *i.e.* 1.4 (with Li) and 1.1 (with Na) $kcal.mol^{-1}$ for DOPA and only about 0.1 (with Li) and 0.4 (with Na) $kcal.mol^{-1}$ for Cl-DOPA.

## *L-DOPA*

PES analysis for *L*-DOPA in the initial state allows the identification of six distinct conformers (*i.e.* local energy-minimum structures) in link with the positioning of the $(CH_2)_2$-$NH_2$-COOH functional group (Fig. SI-8). Among them, three conformations are related to the relative orientation of the $(CH_2)_2$-$NH_2$ group with respect to the 6MR ($\delta_1$-dihedral angle) for a given orientation of the COOH group with respect to $NH_2$ group (structures A, B and C). From these structures, the PES analysis allows determining three further ones (Structures A', B' and C') through a reorientation of the COOH group in nearly opposite orientation with respect to the $NH_2$ group (*cf.* PES evolution linked to the $\delta_2$-dihedral angle). In contrast with DOPA and its halogen-derivative, the most stable structure for the initial form (displayed in Fig. 2) is now obtained for the *o.p.* conformation of the $(CH_2)_2$-$NH_2$ group (Structure B), which is characterized by a ESP minimum of -59.89 in between the two oxygens from carbonyl (and two minima of lower extent (-28.34, -24.11 and 1.92 linked to the functional group)). According to the PES analysis of *L*-DOPA species interacting with $Li^+$ or $Na^+$ or $Mg^{2+}$ in the intermediate and final forms respectively (discussed in SI), the most stable structure is now obtained with an *o.p.* $(CH_2)_2$-$NH_2$ conformation, with nearly opposite orientation to the one found for *L*-DOPA initial state (*i.e.* structure C' $\delta_1 \sim -70.6°$ and $\Delta\delta_1 \sim 173.9$). In these structures, interatomic distances between O-atom and alkaline or Mg species in the bidentate interaction are equal to: 1.86 Å, 2.21 Å and 1.91 Å for Li, Na and Mg-based systems, respectively. The corresponding structures involving one cation with *i.p.* $(CH_2)_2$-$NH_2$ conformation are now unstable. Regarding ESP maps, the main minima are located from each side of the bidentate interaction, with values equal to -41.29 and -39.65, -37.15 and -35.79, -43.31 and -40.29 for $Li^+$, $Na^+$ and $Mg^{2+}$ systems respectively. In agreement with the higher extent in absolute value of these minima values, the most stable final structure is obtained with additional alkaline species interacting with the C=O group of the *o*-quinone ring separated from the $(CH_2)_2$-$NH_2$-COOH chain (conformation B) by the two consecutive CH bonds. For this final form, the interatomic distances between additional alkaline and the O-atom of the carbonyl are about 1.75 Å (Li) and 2.11 Å (Na), respectively while in the preserved bidentate interaction, the couple of alkaline-O interatomic distances are evaluated at (1.79 Å,1.84 Å) with Li and (2.14 Å, 2.19 Å) with Na. For a same conformation of the $(CH_2)_2$-$NH_2$-COOH chain, the structures involving an additional alkaline interacting with the other C=O group of the ring are substantially lowered compared to the most stable structure, with $\Delta G$ of about 0.9 and 0.5 kcal.mol$^{-1}$ for Li- and Na-based systems respectively (*cf.* final forms 2 in Fig. SI-9). A further minimum in the ESP map of the intermediate states located in the vicinity of the carbonyl function from the functional group appears at -32.18 and -34.50 for Li and Na-based systems respectively. This may lead to another possibility of final form for *L*-DOPA, involving a specific interaction of the additional alkaline with the carbonyl the COOH group. Free enthalpy values evaluated for these additional calculated structures (with Li and Na species) is quite comparable with the ones estimated for the former most stable structures. In link with possible conformations of the $(CH_2)_2$-$NH_2$-COOH chain of *L*-DOPA, the analysis of the calculated PES's allows determining other less stable (local energy minimum) structures displayed in Fig. SI-9.

## *CQ*

CQ initial form only presents two local energy-minimum structures associated with the two relative orientations of the -COOH group with respect to the plane of the 6MR. The calculated PES (Fig. SI-10) demonstrate that they are separated by a significant energy barrier of about 5.1 kcal.mol$^{-1}$ whereas both structures (I and II) are characterized by a relative stability of about 1.5 kcal.mol$^{-1}$. The interatomic distances in the bidentate interaction involved for the most stable conformer of the intermediate/final form of CQ interacting with one $Li^+$ or $Na^+$ or $Mg^{2+}$ species is about 1.86 Å, 2.21 Å and 1.91 Å for $Li^+$, $Na^+$, $Mg^{2+}$ compounds, respectively. In the final forms of CQ with $Li^+$ or $Na^+$, two distinct arrangements can again be distinguished according to the side of the additional interaction occurring with the new alkaline cation. The ESP values at the intermediate state are however in favour of a location on the side separated from the functional group by only one H atom, with a value of -31.09/-34.71 against -28.05/-31.52 on the other side for $Li^+/Na^+$, respectively, and this is indeed consistent with the most stable conformer identified after the one-electron process. For these most stable final structures, the involved interatomic distances correspond to 1.75 Å/2.11 Å between the supplementary O and the carbonyl group while they are equal to (1.81 Å,1.84 Å)/(2.16 Å,2.19 Å) I the bidentate interaction for $Li^+/Na^+$ systems, respectively. As for *L*-DOPA, another structure may eventually be considered for this state in which the additional alkaline could potentially interact with the carbonyl of the COOH group, by preserving the bidentate interaction. Nevertheless, this location forces the system to avoid recovering the maximum of stability related to the complete reduction of the quinoidic species (aromatization of the 6MR). Therefore, despite the higher extent of the ESP minima observed in the vicinity of the carboxylate group (-41.41 and -44.58 for $Li^+/Na^+$ systems, respectively, compared to the values in the vicinity of the redox centres), the structures with additional alkaline ion interacting with C=O of the COOH group are found to be significantly less stable with $\Delta$G differences compared to the most stable structures evaluated at about 9.8 and 8.1 kcal.mol$^{-1}$, for Li- and Na-based systems, respectively. As for *L*-DOPA, the PES analysis allows determining other local energy minimum structures but which are significantly less stable compared to the other conformers of CQ displayed in Fig. SI-11.

## HMQ

In a similar manner to the case of DOPA and Cl-DOPA, initial state of HMQ exhibits three local energy-minimum structures due to conformational modulation of the $CH_2$-OH group with respect to the plane of the 6MR (*cf.* PES in Fig. SI-12). Accordingly, the *i.p.* $CH_2$-OH conformation corresponds to the most stable structure (A) compared to both *o.p.* conformations (B and C, see SI). In contrast, for intermediate and final forms, the most stable calculated structures interacting with $Li^+$, $Na^+$ or $Mg^{2+}$ species are found with an *o.p.* $CH_2$-OH conformation, for which we observe again an ESP minimum in between the two carbonyl groups, of -57.70. The interatomic distances characterizing the bidentate interaction between O atoms and the alkaline or $Mg^{2+}$ ion are respectively equal to 1.86 Å (Li), 2.21 Å (Na), and 1.90-1.91 Å (Mg). Among the two distinct potential positionings for the further $Li^+$ or $Na^+$ cation, the most stable final structure (form I) is obtained with the additional alkaline ion interacting with the C=O group of the ring separated from the attached $CH_2$-OH chain by only one CH bond. In the secondary structure (Final Form II), the additional alkaline interacts instead on the other side. The Gibbs free energy difference $\Delta$G between both forms is however quite small, of about 0.6 and 0.1 kcal.mol$^{-1}$ for $Li^+$ and $Na^+$ cases, respectively (*c.f.* Fig.SI-13). This could explain (like in the case of Cl-DOPA) that the low difference in ESP minima of the intermediate phase (*i.e.* -32.40 and -34.31 in the case of Li-compound or -38.39 and -36.21 for the Na-system) could not discriminate sufficiently the two positionings. In both final forms, the interatomic distance between additional alkaline and the O-atom is evaluated at about 1.75 Å (Li) and 2.12 Å (Na), respectively. Compared to the intermediate form, the alkaline-O interatomic distances in the bidentate bonding are again affected by the presence of this additional cation, by introducing a slight asymmetry: *i.e.* interatomic distances equal to (1.79 Å,1.84 Å) with Li and (2.15 Å, 2.19 Å) with Na.

## 1.2 Figures SI-1 to SI-4

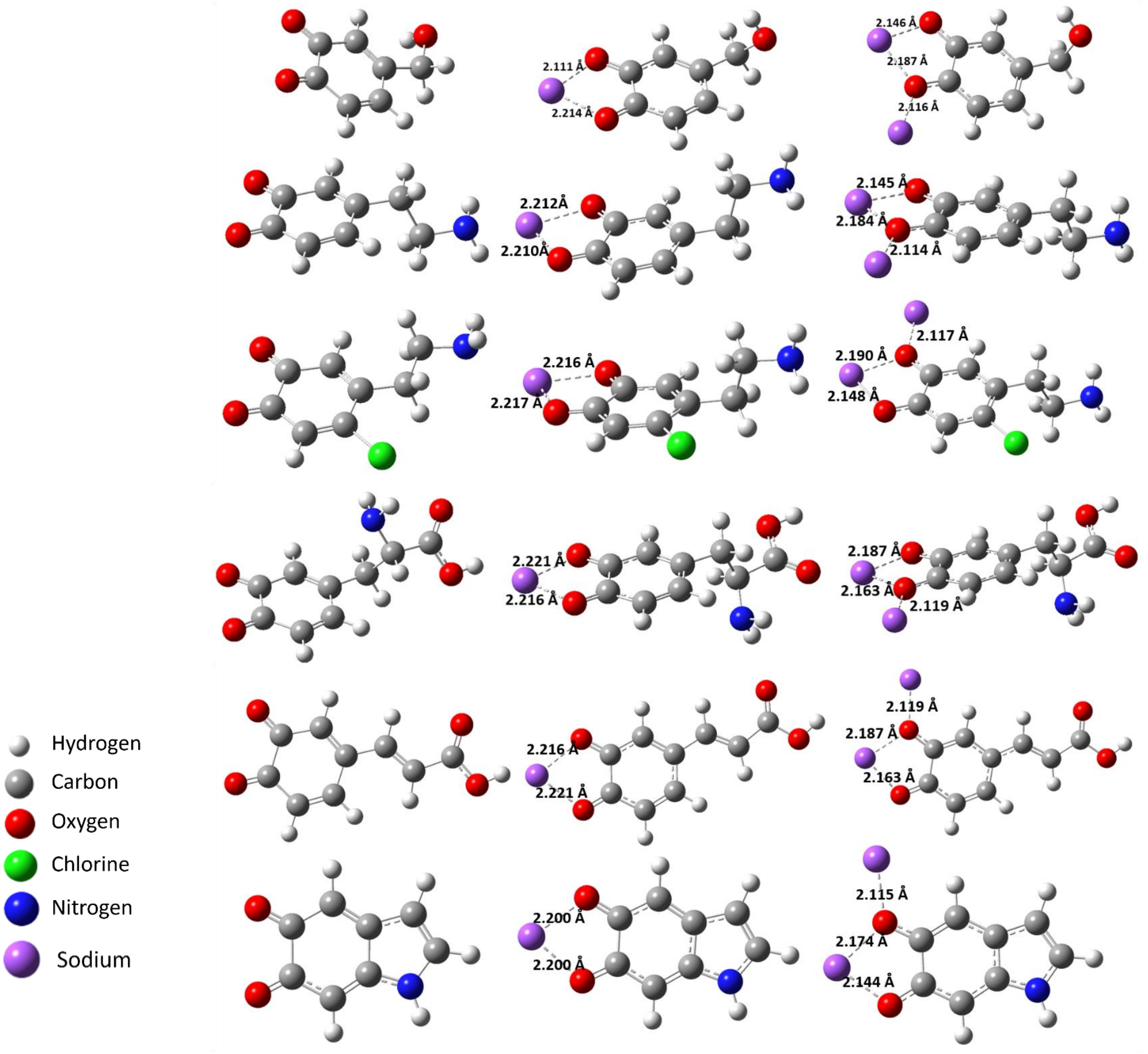

**Fig. SI-1:** Most stable structures for Na-based systems. Left: monomer (initial state); Middle: complex involving one $Na^+$ cation (Single reduction); Right: complex involving two $Na^+$ cations (Double reduction); From Top to Bottom: HMQ, DOPA, Cl-DOPA, *L*-DOPA, CQ and IQ.

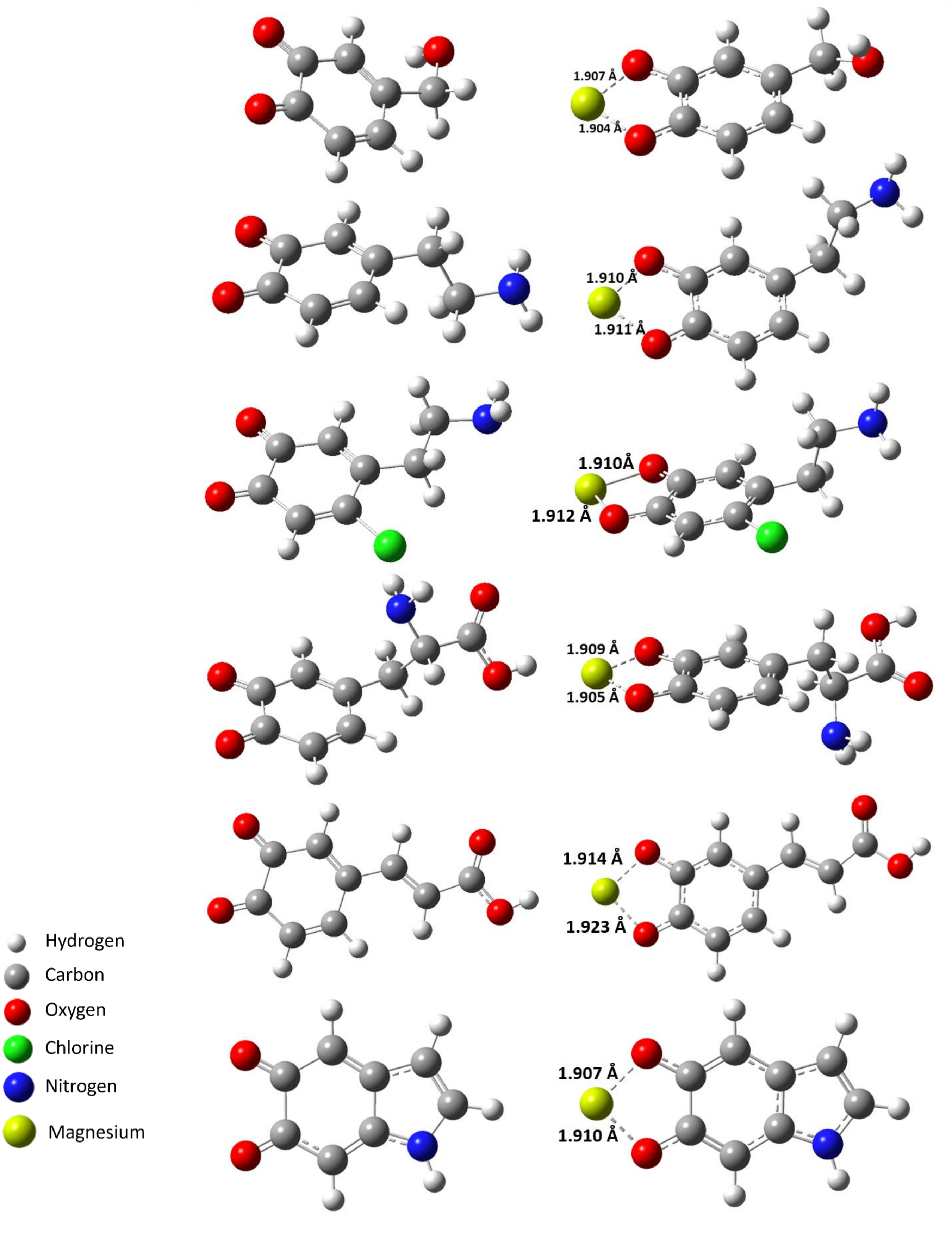

**Fig. SI-2:** Most stable structures for Mg-based systems. Left: monomer (initial state); Right: complex involving one $Mg^{2+}$ cation (Double reduction); From Top to Bottom: HMQ, DOPA, Cl-DOPA, *L*-DOPA, CQ and IQ.

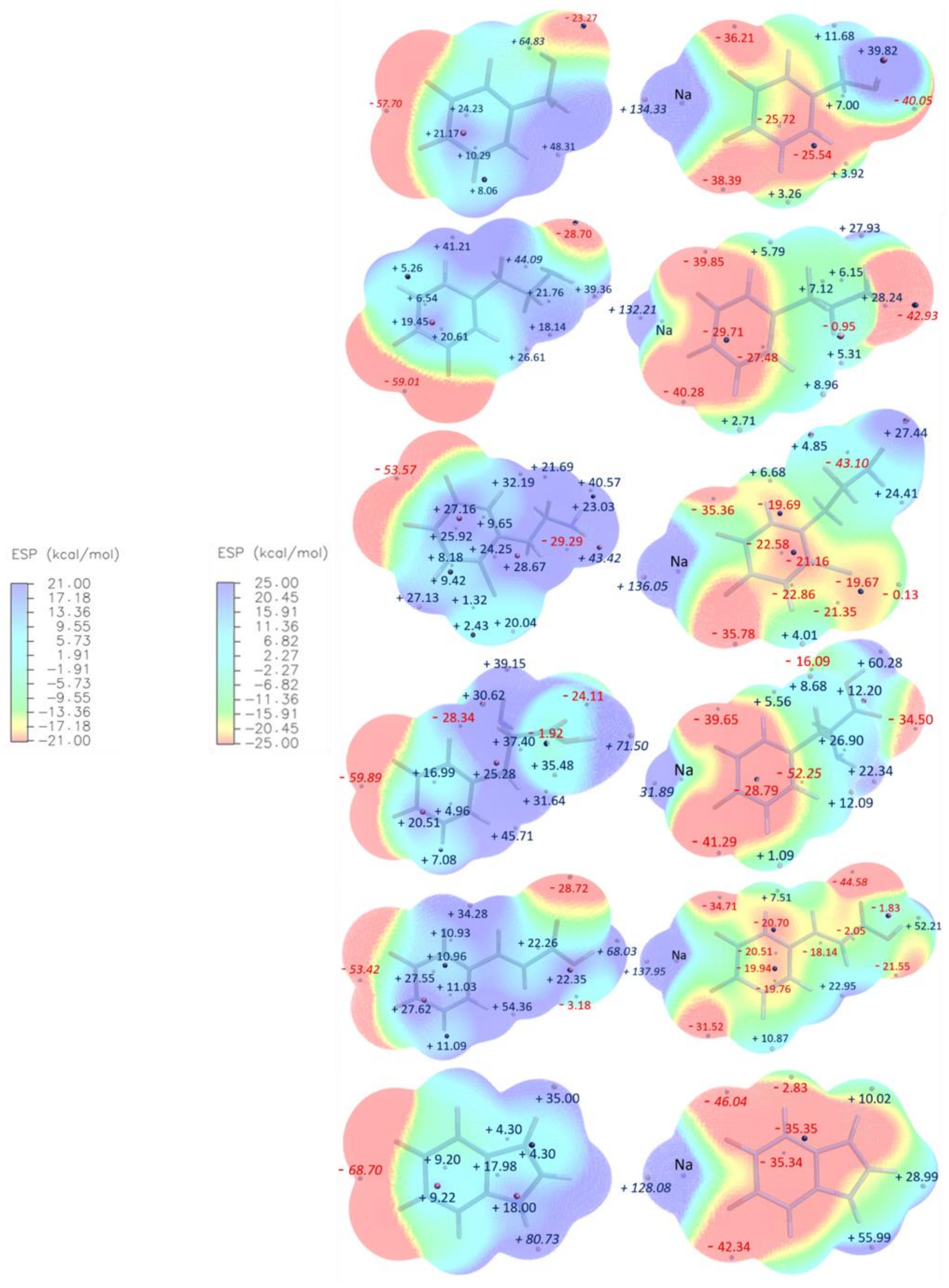

**Fig. SI-3:** ESP maps for the initial and intermediate forms of Na-based systems. Left: initial state; Middle: complex involving one Na$^+$ cation (Single reduction); From Top to Bottom: HMQ, DOPA, Cl-DOPA, *L*-DOPA, CQ and IQ. The colour scale applies to: Left: Initial forms and Final form of HMQ, DOPA, Cl-DOPA, and *L*-DOPA; Right: Final form of IQ.

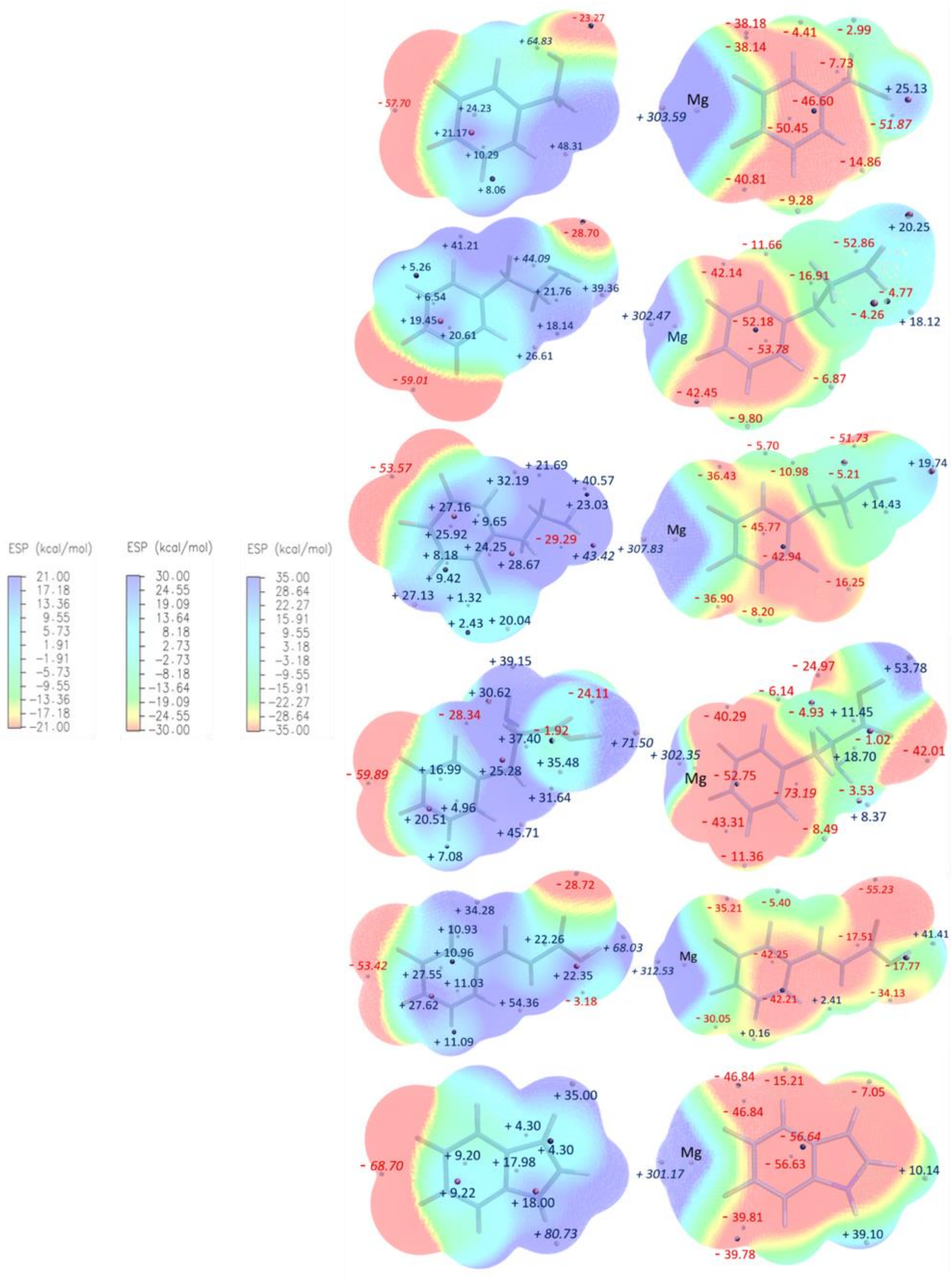

**Fig. SI-4:** ESP maps for the initial and final forms of Mg-based systems. Left: initial state; Right: complex involving one $Mg^{2+}$ cation (*i.e.* final state after Double reduction); From Top to Bottom: HMQ, DOPA, Cl-DOPA, *L*-DOPA, CQ and IQ. The colour scale applies to: Left: Initial forms and Final form of *L*-DOPA; Middle: Final form of HMQ; Right: Final form of DOPA, Cl-DOPA, CQ, and IQ.

## 1.3 Presentation of secondary structures and PES – Figures SI-5 to SI-13

### *IQ*

The secondary (stable) structures (Final form II) calculated for IQ interacting with $Li^+$ or $Na^+$ are displayed in Fig. SI-5.

**A) with $Li^+$**

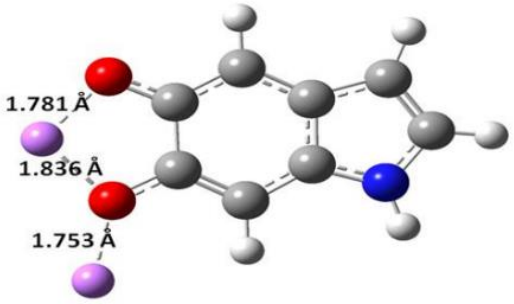

**B) with $Na^+$**

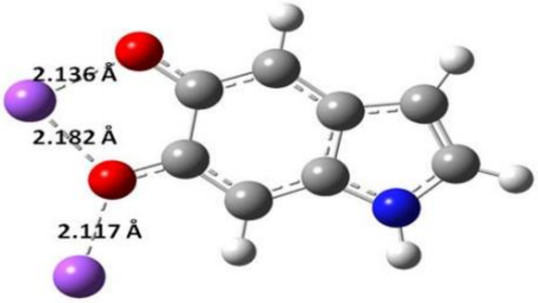

**Fig. SI-5:** Secondary (stable) structures (Final form II) calculated for IQ.

### *DOPA and Cl-DOPA*

DOPA and Cl-DOPA molecules are characterized by three conformers with respect to the orientation of the $(CH_2)_2$-$NH_2$ group relatively to the plane of the *o*-quinone ring. The corresponding calculated PES are displayed in Fig. SI-6.

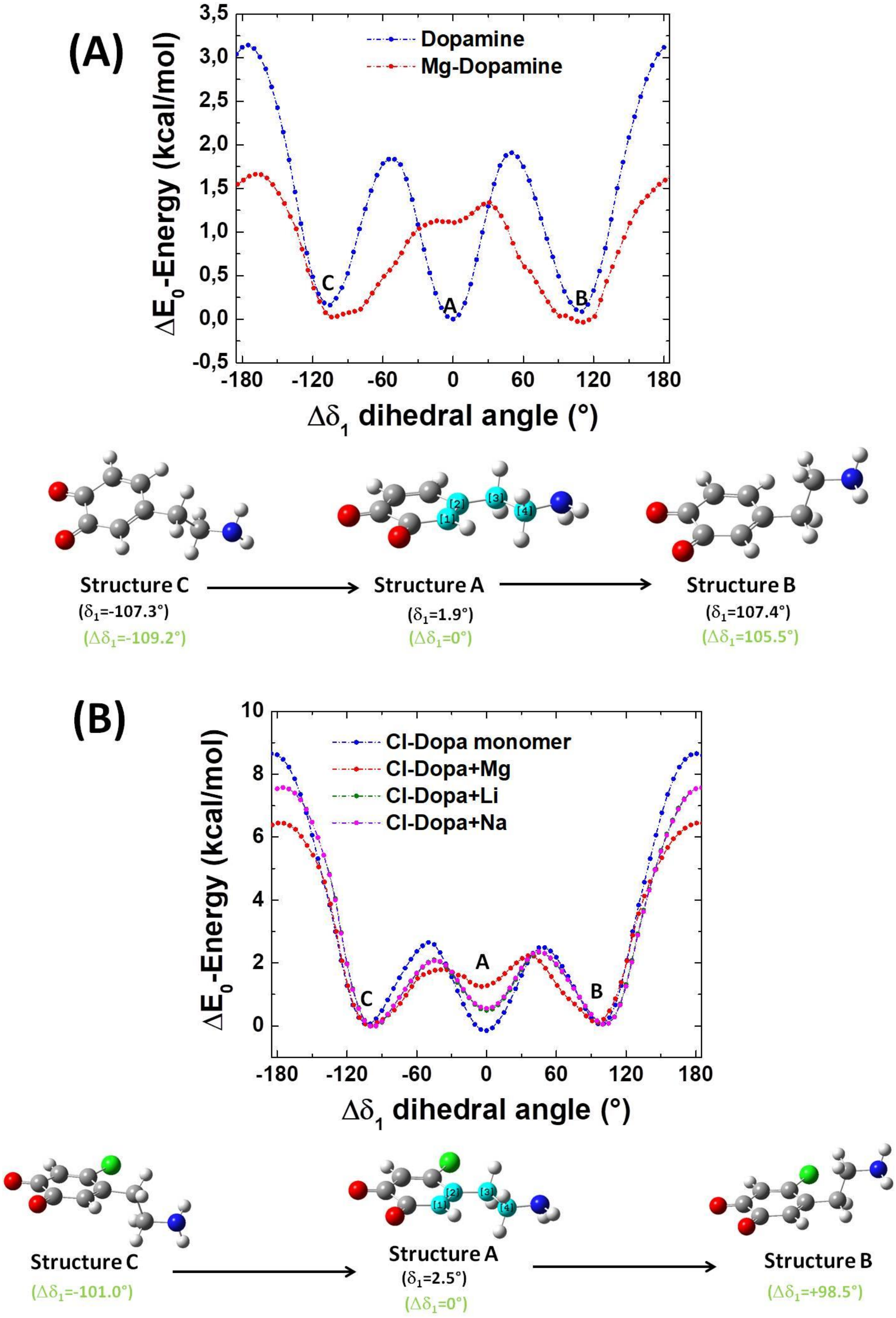

**Fig.SI-6**: Evolution as a function of the dihedral angle $\delta_1$ (defined by highlighted atoms in the Structure A) of the PES for DOPA (A) and Cl-DOPA (B) in the initial (monomer) and intermediate forms.

For both compounds, the most stable initial state corresponds to the $(CH_2)_2$-$NH_2$ group nearly situated in the plane of the 6MR. In contrast, for the intermediate form, the structures with o.p. $(CH_2)_2$-$NH_2$ conformations become more stable than that with i.p. $(CH_2)_2$-$NH_2$ conformation (*c.f.* PES in Fig. SI-6). Independently of the nature of the atom interacting with the *o*-quinone ring, the most stable structure is obtained with o.p. conformation B (Fig. 2 and SI-1/SI-2). The other calculated secondary final forms (II) calculated for DOPA and Cl-DOPA are displayed in Fig. SI-7.

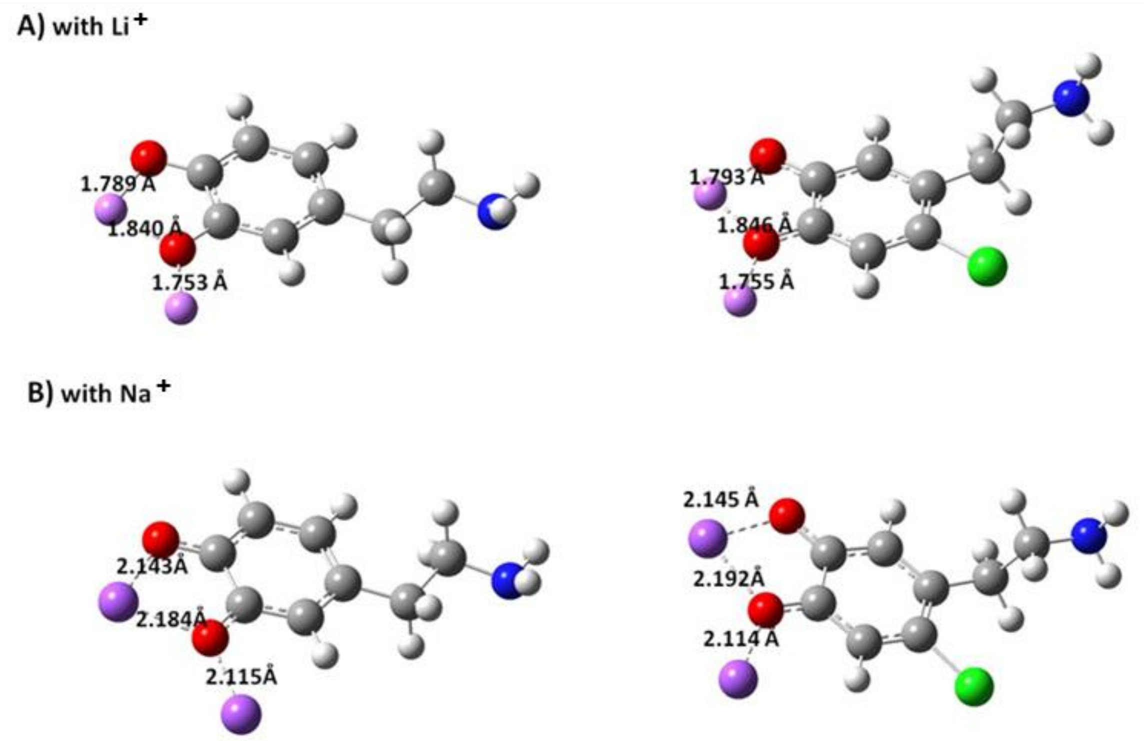

**Fig.SI-7:** Secondary final forms (II) calculated for DOPA and Cl-DOPA.

## *L-DOPA*

The analysis of the calculated PES (Fig. SI-8) for *L*-DOPA in the initial state (monomer) allows the identification of six distinct conformers (local energy-minimum structures) in link with the orientation of the $(CH_2)_2$-$NH_2$-COOH group attached to the 6MR. Three conformations are resulting from the relative orientation of the $(CH_2)_2$-$NH_2$ group with respect to the *o*-quinone ring ($\delta_1$-dihedral angle) for a given orientation of the COOH group relative to $NH_2$ one (structures A, B and C). From these structures, the PES analysis allows determining three supplementary configurations (Structures A', B' and C') by reorientation of the COOH group in nearly opposite orientation with respect to the $NH_2$ one.

For *L*-DOPA interacting with $Mg^{2+}$ species (Fig. SI-8A), the most stable structure is now obtained with an o.p. $(CH_2)_2$-$NH_2$ conformation nearly in opposite orientation compared to the one characterizing the *L*-DOPA monomer. Such a trend is also observed for *L*-DOPA interacting with $Li^+$ or $Na^+$. Only structures with o.p. $(CH_2)_2$-$NH_2$ conformations can be related with a local minimum energy whereas the structures involving i.p. $(CH_2)_2$-$NH_2$ conformation are now unstable (Fig. SI-9).

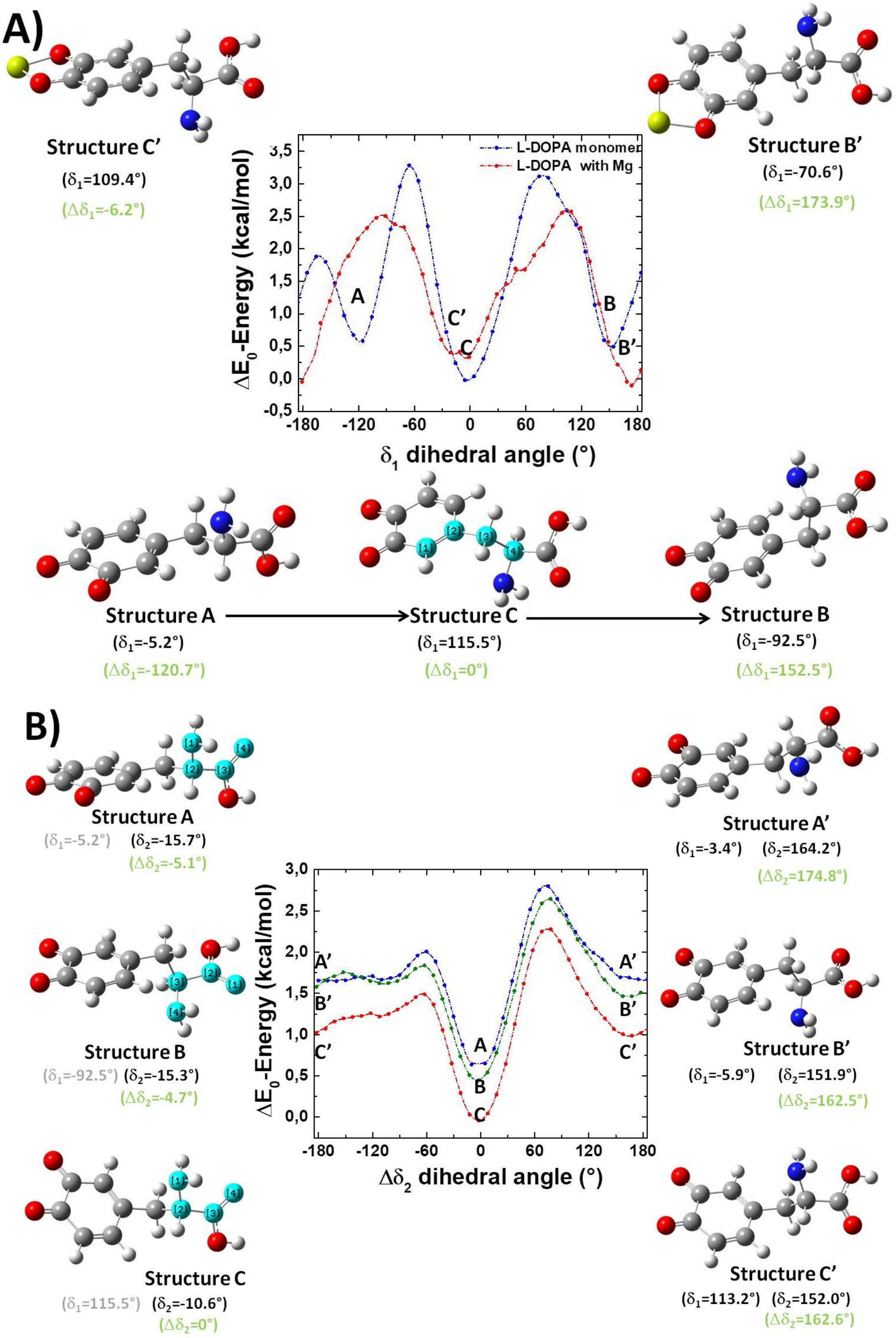

**Fig.SI-8**: Evolution as a function of the dihedral angle $\delta_1$ and $\delta_2$ (defined by highlighted atoms) of the PES for *L*-DOPA. (A) PES as a function of $\delta_1$ evolution for *L*-DOPA in the initial and final state involving $Mg^{2+}$. (B) Evolution of the PES as a function of the $\delta_2$ dihedral angle for the *L*-DOPA monomer from conformers A, B and C.

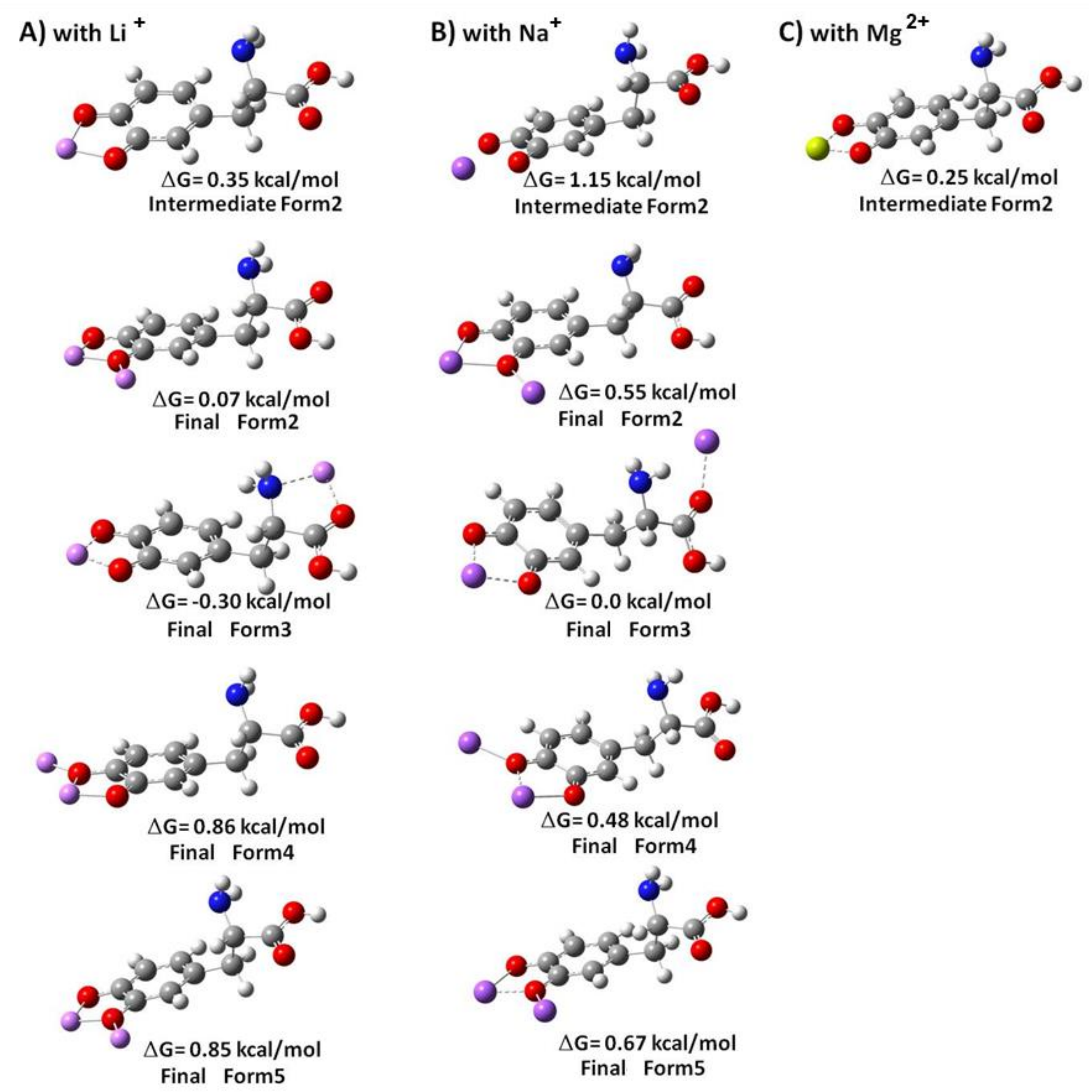

**Fig.SI-9**: Secondary (stable) structures for reduced *L*-DOPA interacting with $Li^+$ and $Na^+$ (intermediate and final forms) and with $Mg^{2+}$ (final form). ΔG values indicate the Gibbs free energy difference (at 298K) between the considered structure and the corresponding most stable conformer (Final Form I) displayed in Fig. 3.

## *CQ*

The PES evolution (Fig. SI-10) as a function of the relative orientation for the COOH group with respect to the 6MR plane ($\delta_2$-dihedral angle) demonstrates that CQ initial state is characterized by two conformers well-separated by a significant energy barrier (about 5.1 kcal.mol$^{-1}$).

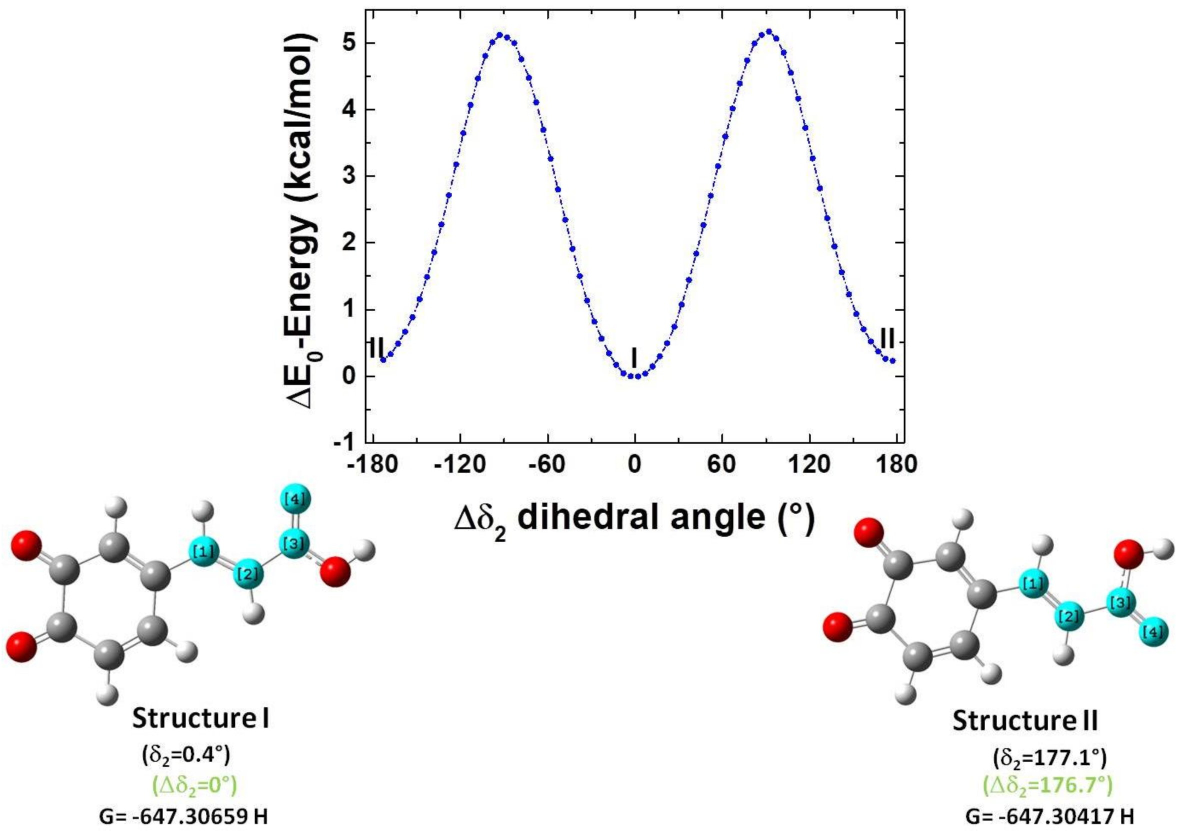

**Fig. SI-10**: Evolution of the PES as a function of the dihedral angle $\delta_2$ (defined by highlighted atoms) for the CQ compound.

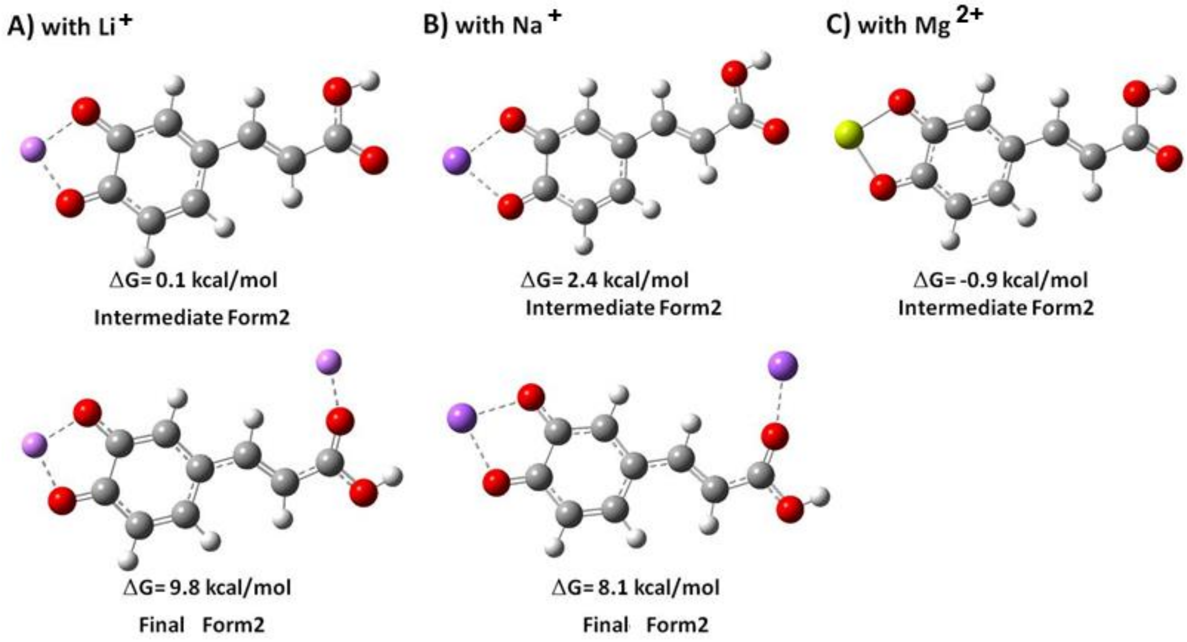

**Fig. SI-11**: Secondary (stable) structures for reduced CQ interacting with $Li^+$ or $Na^+$ (intermediate and final forms) and with $Mg^{2+}$ (final form). ΔG values indicate the Gibbs free energy difference (at 298K) between the considered structure and the most stable conformer displayed in Fig. 3.

## *HMQ*

The PES analysis (Fig. SI-12) indicates that HMQ initial state presents three local energy-minimum structures (conformers) resulting from various orientations of the $CH_2$-OH group with respect to the 6MR plane. The most stable structure (A) is related to the *i.p.* $CH_2$-OH conformation whereas both other structures of HMQ monomer present *o.p.* conformations (B and C).

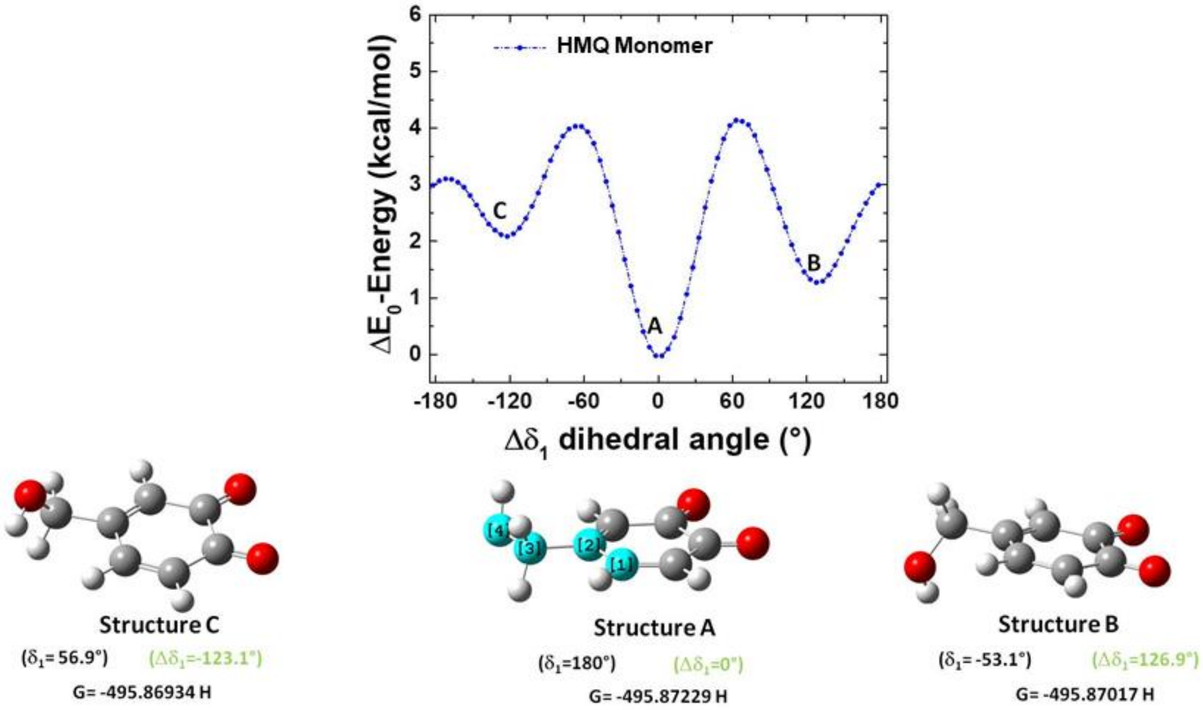

**Fig. SI-12**: Evolution of the PES as a function of the dihedral angle $\delta_1$ (defined by highlighted atoms) for the HMQ compound.

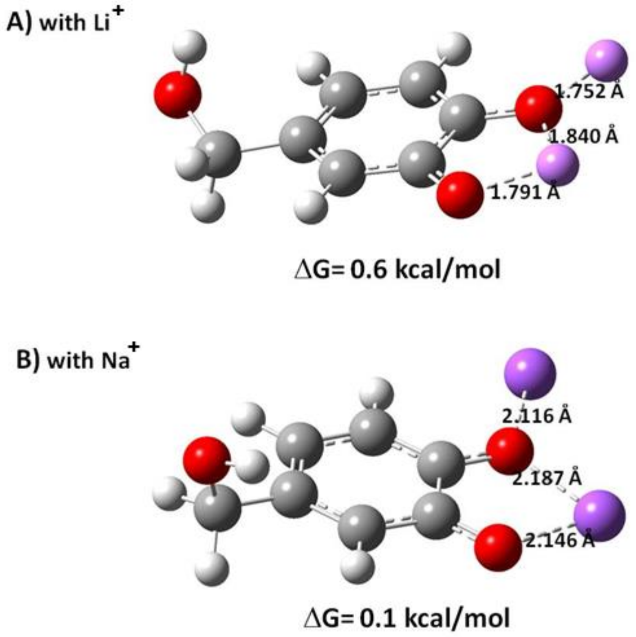

**Fig. SI-13**: Secondary (stable) final structures for reduced HMQ interacting with $Li^+$ or $Na^+$ (final forms). ΔG values indicate the Gibbs free energy difference (at 298K) comparatively to the most stable conformer displayed in Fig. 3.